

UNCLASSIFIED

SECURITY CLASSIFICATION OF THIS REPORT

AD-A205 039

ITIC FILE COPY

(2)

REPORT DOCUMENTATION NUMBER

READ INSTRUCTIONS
BEFORE COMPLETING FORM
PERFORMING ORGANIZATION'S CATALOG NUMBER

1. REPORT NUMBER

ARO 24623.7-EG-UIR

N/A

N/A

4. TITLE (and Subtitle)

Fuel Impingement in a Direct Injection Diesel Engine

5. TYPE OF REPORT & PERIOD COVERED

Reprint

6. PERFORMING ORG. REPORT NUMBER

N/A

7. AUTHOR(s)

8. CONTRACT OR GRANT NUMBER(s)

DAAL03-86-K-0174

9. PERFORMING ORGANIZATION NAME AND ADDRESS

University of Wisconsin
Madison, Wisconsin 53705

10. PROGRAM ELEMENT, PROJECT, TASK AREA & WORK UNIT NUMBERS

N/A

11. CONTROLLING OFFICE NAME AND ADDRESS

U. S. Army Research Office
P. O. Box 12211
Research Triangle Park, NC 27709

12. REPORT DATE

1988

13. NUMBER OF PAGES

14

14. MONITORING AGENCY NAME & ADDRESS (if different from Controlling Office)

15. SECURITY CLASS. (of this report)

Unclassified

15a. DECLASSIFICATION/DOWNGRADING SCHEDULE

16. DISTRIBUTION STATEMENT (of this Report)

Submitted for announcement only.

DTIC
ELECTE
JAN 23 1989
S D
C/D

17. DISTRIBUTION STATEMENT (of the abstract entered in Block 20, if different from Report)

18. SUPPLEMENTARY NOTES

The view, opinions, and/or findings contained in this report are those of the author(s) and should not be construed as an official Department of the Army position, policy, or decision, unless so designated by other documentation.

19. KEY WORDS (Continue on reverse side if necessary and identify by block number)

20. ABSTRACT (Continue on reverse side if necessary and identify by block number)

ABSTRACT ON REPRINT

DISTRIBUTION STATEMENT A
Approved for public release
Distribution Unlimited

SAE The Engineering Society
For Advancing Mobility
Land Sea Air and Space®

400 COMMONWEALTH DRIVE WARRÉNDALÉ, PA 15096

SAE Technical Paper Series

881316

Fuel Impingement in a Direct Injection Diesel Engine

J. Naber, B. Enright and P. Farrell

Engine Research Center
Univ. of Wisconsin-Madison

Accession For	
NTIS CRA&I	<input checked="" type="checkbox"/>
DTIC TAB	<input type="checkbox"/>
Unannounced	<input type="checkbox"/>
Justification	
By	
Distribution /	
Availability Codes	
Dist	Avail and/or Special
A-1 Z1	

DTIC
COPY
INSPECTED
6

International Off-Highway & Powerplant
Congress and Exposition
Milwaukee, Wisconsin
September 12-15, 1968

The appearance of the code at the bottom of the first page of this paper indicates SAE's consent that copies of the paper may be made for personal or internal use, or for the personal or internal use of specific clients. This consent is given on the condition, however, that the copier pay the stated per article copy fee through the Copyright Clearance Center, Inc., Operations Center, P.O. Box 765, Schenectady, N.Y. 12301, for copying beyond that permitted by Sections 107 or 108 of the U.S. Copyright Law. This consent does not extend to other kinds of copying such as copying for general distribution, for advertising or promotional purposes, for creating new collective works, or for resale.

Papers published prior to 1978 may also be copied at a per paper fee of \$2.50 under the above stated conditions.

SAE routinely stocks printed papers for a period of three years following date of publication. Direct your orders to SAE Order Department.

To obtain quantity reprint rates, permission to reprint a technical paper or permission to use copyrighted SAE publications in other works, contact the SAE Publications Division.



All SAE papers are abstracted and indexed in the SAE Global Mobility Database.

SAE GLOBAL MOBILITY DATABASE

No part of this publication may be reproduced in any form, in an electronic retrieval system or otherwise, without the prior written permission of the publisher.

ISBN 9148-7191

Copyright © 1998 Society of Automotive Engineers, Inc.

Statements and opinions advanced in this paper are those of the author(s) and not necessarily those of SAE. The author is solely responsible for the content of the paper. A process is available by which discussions will be placed with the paper if it is published in SAE Transactions. For permission to publish this paper in full or in part, contact the SAE Publications Division.

Persons wishing to submit papers to be considered for presentation or publication through SAE should send the manuscript or a 300 word abstract of a proposed manuscript to: Secretary, Engineering Activity Board, SAE.

Printed in U.S.A.

Fuel Impingement in a Direct Injection Diesel Engine

J. Naber, B. Enright and P. Farrell

Engine Research Center
Univ. of Wisconsin-Madison

ABSTRACT

High injection pressure impinging spray experiments and modeling were performed under simulated diesel engine conditions (pressure and density) at ambient temperature. A spray impinged normal to a small crown in the bowl of a simulated piston. High speed photography was used in the constant volume bomb to examine the effect of impingement on fuel mixing. The spray model which includes drop breakup, coalescence, impingement, and vaporization effects was used to predict fuel mixing in the bomb. The spray distributions predicted by the model are compared to the photographs obtained in the bomb. reprints.

SPRAY IMPINGEMENT BACKGROUND

Interest in direct injection stratified charge engines and direct injection diesel engines has included strong interest in developing accurate models for liquid fuel sprays. Among the more widely used models is KIVA, a code developed at Los Alamos National Laboratory [1]. Recent developments have focussed on modeling basic gas phase fluid mechanics and using liquid spray submodels to describe the behavior of the liquid spray. The detailed spray submodels have primarily focussed on improved modeling of drop breakup [2,3], drop coalescence [4], and improved descriptions of the initial conditions and boundary conditions applied to the problem [4]. The results of this work have been evaluated by comparison with limited

amounts of data for sprays in regions far from the injector ($>200d$ where d is the injector orifice diameter). These results have emphasized the significance of the combination of drop breakup and coalescence, and the relative insensitivity of far field drop size, velocity, and spread angle results to the injection conditions. In addition to studies of liquid sprays in a semi-infinite gas field, model results have been extended to finite gas fields where the spray impinges on a solid surface at some location relatively far from the injector tip ($>200d$). A recent paper by Naber and Reitz [5] has addressed this issue by examining the problem of a diesel spray impinging on the bowl of a piston in a moderate swirl engine. Comparison of their results with photographs from an operating engine indicate good qualitative agreement between their model predictions for overall far-field spread and apparent surface wetting and the data acquired from the photographs.

In some combustion situations of interest, the geometry of the combustion chamber may limit the extent of the spray to regions of significantly smaller l/d values than those for which model results have been established. In these near field regions, the issues of spray behavior near the nozzle tip and the effects of high velocity liquid sprays impinging on solid surfaces may be significant.

Proposals for relatively novel cylinder geometries, in particular novel piston

* Numbers in brackets designate references listed at the end of this paper.

8146-7131/82/0012-1316\$02.50

Copyright 1982 Society of Automotive Engineers, Inc.

①

geometries, have recently been made by Kroeger [6] and Kato and Onishi [7]. These chamber designs generally include a piston with a bowl and a small projection in the middle of the bowl. These piston top geometries appear to have been developed for somewhat different applications: Kroeger's (Caterpillar) for direct injection diesels using neat methanol, and Kato and Onishi's (NiCE) for direct injection stratified charge (DISC) engines. The basic geometry exhibits a raised surface at or near the center of the piston bowl, onto which some or all of the fuel spray impacts. In the case of the Caterpillar engine, nine other spray lobes are also injected in a normal pattern radially and slightly downward from the injector. In the case of the NiCE engine all of the fuel is sprayed onto the raised piston impingement area from a single orifice. In either case the liquid which impacts the raised surface is expected to provide a centrally located cloud of fuel drops and fuel vapor which will enhance the subsequent combustion event. In both cases, the intent of the piston projection is to enhance the fuel injection process by directing some or all of the fuel to be injected onto the projection. This projection is typically 15-20 nozzle orifice diameters downstream of the nozzle tip, which puts it in a region of the very near spray field where liquid velocities are quite high. Improved performance or continued performance under atypical operating conditions were demonstrated experimentally in both of these engines. In general, this is a very different situation from the conditions of previous work in spray modeling, yet it presents an area of particular interest in terms of analyzing the performance of significantly different combustion and fuel injection geometries. These new geometries may present a particular challenge to existing codes, as they include physical effects not explicitly modeled in many current codes, such as detailed wall interactions, wall-induced breakup, and wall spray deflection.

To date the issue of wall impingement effects on liquid fuel spray in the near field of the spray has not been extensively studied experimentally. It is not clear that current spray models will be able to accurately handle this type of spray impingement problem in their current state.

This paper presents the application of one currently available spray code (KIVA) to the situation of the piston geometry displayed by the engines presented by Kroeger [6] and by Kato and Onishi [7]. A set of experiments has been performed for the raised piston center section geometry using a high pressure diesel fuel injector in a high pressure unheated bomb. High speed movies provided information on the spread and location of the spray under different operating conditions. The results from the movies are compared to the results of the computer model in its original state, and in a modified state.

NUMERICAL MODEL

A three dimensional finite difference numerical model (KIVA) was used to model the spray in the constant volume bomb. The model solves the gas phase using a time explicit eulerian finite difference scheme for the averaged Navier-Stokes equations with a $k-\epsilon$ turbulence model. For this application, the geometry of the spray was considered axisymmetric, so a two-dimensional version of the code was used. The spray is modeled using a stochastic lagrangian scheme where parcels represent a number of drops with common properties. The parcels interact with the gas through terms in the gas equations exchanging mass, momentum, and energy, and generating turbulence. Drop coalescence, breakup and impingement are included in the stochastic parcel model. More details of the numerical model are given in the references [1,2,5,8].

The breakup model used in this study is described in detail by Reitz and Diwakar [8]. The initial parcel diameter at the time of injection is equal to the nozzle diameter. This differs from their earlier work [2] and that of Amden et al. [1] where the initial parcel diameters were determined from distributions. Amden's [1] probability distribution normalized to unit total weight is

$$g(r) = \frac{r^3}{2 r_{32}^4} e^{-3r/r_{32}} \quad (1)$$

Where r_{32} is the Sauter mean radius. With a small initial diameter at injection the combined effects of drop breakup and

coalescence determines the drop distribution downstream of the injector. Two modes of drop breakup bag and stripping are modeled. Bag breakup occurs for

$$We = \frac{\rho_f V_{inj}^2 r}{\sigma} > 6 \quad (2)$$

and stripping breakup for

$$\frac{We}{\sqrt{Re}} > 0.5$$

$$Re = \frac{2 V_{inj} r}{\nu} \quad (3a,3b)$$

The impingement of drops on solid boundaries is modeled using an analogy with potential flow jet impingement as described by Naber and Reitz [5]. The drop leaves tangent to the surface in a direction determined from a probability distribution function. The probability distribution function is derived from potential flow jet conservation of mass and momentum and an assumed momentum distribution. The angle ψ is the angle of the tangential velocity of the parcel after collision with the wall in the plane of the surface, relative to the impinging tangential velocity vector. The parcel's new velocity vector direction is determined from the equation

$$\psi = -\frac{\pi}{\beta} \ln \{ 1 - \chi (1 - e^{\beta}) \} \quad (4)$$

where χ is a uniform random number (0,1), and β is determined from the function

$$\sin(\alpha) = \left[\frac{e^{\beta} + 1}{e^{\beta} - 1} \right] \frac{1}{1 + (\pi/\beta)^2} \quad (5)$$

Here α is the impingement angle measured from the surface normal. The parcel does not change its diameter due to the wall impingement.

For each operating condition of interest, the model requires specification of the initial

conditions and boundary conditions. For the gas flow, the initial condition is a uniform field of a known pressure and density. The initial gas velocity is zero and the temperature is a constant throughout the problem, as the bomb is operated at room temperature and vaporization is neglected in the model. For the spray, an initial drop size or distribution, initial velocity, and spread angle must be specified. As the initial drop size was varied during the course of the work, discussion of the actual values used is included in the discussion of the model results. Exponentially decaying spray velocity profiles were estimated using the known peak (initial) fuel pressures, injector closing pressures, injection durations, fuel delivery, and orifice discharge coefficients provided by the injector manufacturer [9]. The initial spray angle was chosen from the photographs of the spray. The grid used in the computations is shown in Fig. 1. A single azimuthal sector of 0.5 degrees was used for the axisymmetric geometry with 17 radial and 13 axial grid points. A typical run with this model took about 30 minutes of computer time on a Cray XMP.

For each set of conditions modeled, the output consists of a series of plots at various times, providing the current location of the spray parcels, liquid and vapor concentration contours, and temperature contours. In this paper only the spray parcel location plots will be displayed.

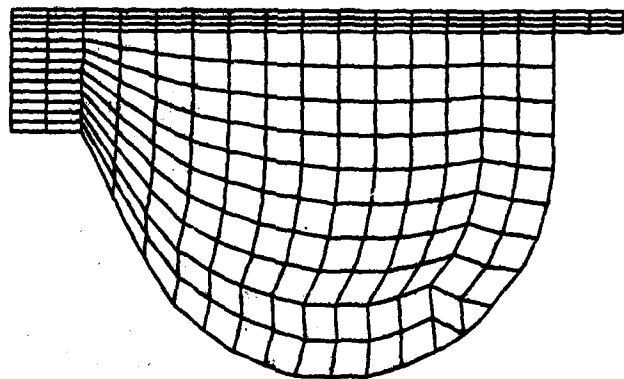


Fig.1. Axisymmetric computational grid. Domain used for calculation of impinging spray in constant volume bomb.

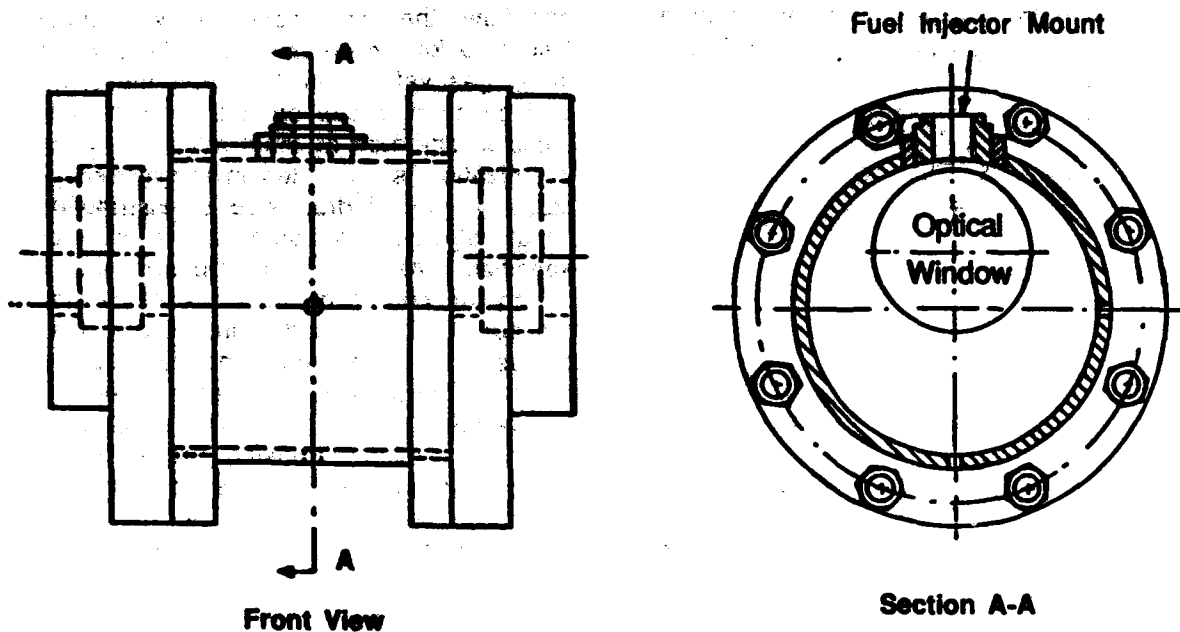


Fig. 2. Front and section views of pressurized bomb with optical access. End caps orientated to view top portion of chamber.

CONSTANT VOLUME BOMB EXPERIMENTS

A constant volume bomb was constructed to provide a chamber capable of providing the high gas pressures and densities common in high compression ratio engines. A sketch of the constant volume bomb is given in Fig. 2. The bomb was constructed of 203 mm (8 in.) diameter pipe, 203 mm (8 in.) long. At each end of the pipe, a flange was welded on and a cap fitted to the end. In the caps on each end were mounted 101 mm (4 in.) quartz windows. The window arrangement was designed to allow the end caps to be remounted in a variety of positions to allow a view of various portions of the spray. At the center, axially, of the chamber, a mounting flange was welded into the side wall for mounting the fuel injector. The position of the injector and tip were adjustable to some extent to ensure the shape of the volume played little role in the subsequent spray motion. The chamber has been statically tested to 4.1 MPa, and is typically operated at about 2.1 MPa gas pressure.

The fuel injector used in this series of experiments was an electronically controlled BKM injector from Servojet Products with a

single hole 0.406 mm diameter nozzle and a maximum peak fuel pressure greater than 138 MPa. This injection system exhibited a rapid needle lift to introduce the fuel at a pressure near the peak fuel pressure. Peak pressure was reached almost instantaneously, and dropped steadily until a preloaded spring ended injection. The quantity of fuel injected is determined by the injector geometry and the fuel rail pressure. Fig. 3 shows a representative injection pressure profile taken from [9] for this type of injector.

The pressure and density in the bomb were chosen to match that of a test engine at 15 degrees btdc ($P_g=32.0$ atm, $\rho_g=14.9$ Kg/m³ at $T=760$ K) by using a mixture of 0.30 N₂ and 0.70 He by volume. Table 1 lists injector conditions for the three events photographed. The fuel used in all of the experiments was standard type I referee fuel.

The time varying extent of the fuel spray was measured in the bomb using a high speed movie camera running at 5000 frames per second. A copper-vapor laser providing pulses approximately 10 ns long, at repetition rates up to 10 kHz was used as a light source. For this experiment the laser and camera were synchronized to allow one laser pulse per

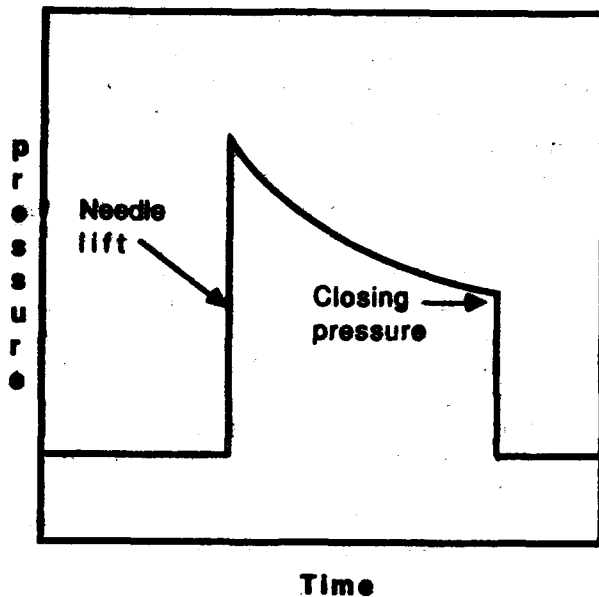


Fig. 3. Typical injector pressure profile of BKM injector showing rapid needle lift to peak pressure.

frame during the entire film sequence. Timing marks on the film allow estimates of the actual film speed at any time.

For this series of experiments a piston surface similar in general shape to the piston crowns indicated by Kroeger [6] and by Kato and Onishi [7] was constructed. In order to allow optical access, a truncated piston surface, as shown in Fig. 4a was constructed. The land diameter was 8.76 mm, and the bowl diameter was 67.3 mm with a maximum depth of 21.6 mm. The injector was placed 6.43 mm above the land on the cusp, providing a distance from the injector tip of 16 times the orifice diameter. A flat plate was attached 3.0 mm above the tip of the injector to simulate the head in an engine. To expose the spray, the front and back of the piston bowl were milled flat to the bottom of the bowl, leaving a center section 40.4 mm wide.

The spray was back lighted using the copper vapor laser beam which was expanded and collimated through a set of lenses and then diffused at the entrance window of the bomb. A Photec 16 mm camera with a 90 mm f/4 lens was used to expose 100 ft of 400 ASA film. The photographic setup is shown in Fig. 4b.

	LOW	MED.	HIGH
Rail Pres. (MPa)	4.7	6.1	7.8
Peak Pres. (MPa)	83	91	116
Vol. of Fuel Inj. (mm ³)	35	69	104
Duration (ms)	1.00	1.92	2.75
Ave. Vel. (m/s)	267	279	292

Table 1. Experimental Conditions

The resulting films were analyzed frame by frame using a 512 by 512 CCD video camera connected to a frame grabber board in a microcomputer. The digitized frames were processed using a Sobel edge filter [10] for finding the edge of the spray, a 2-D median filter to reduce image noise, and thresholding to improve final image contrast. The result of the image processing is a two level image of the spray and chamber edges. The spray edges determined by this procedure were then compared to the parcel location pattern predictions provided by the model at the same operating conditions for the same time from the start of injection.

RESULTS

The model was run as described above for the set of conditions used in the constant volume bomb. A typical result for the "standard" model is shown in Fig. 5a where the liquid drop parcel locations predicted by the model are indicated by the circles. Open circles indicate parcels whose drops have not hit any solid surface. The parcel size is representative of the relative size of the drops in the parcel, although these are rescaled for each figure, so size evaluations from figure to figure are not always valid. The solid line in the figure indicates the outer boundary of the spray obtained from the processed high speed movies at the same conditions and time from injection

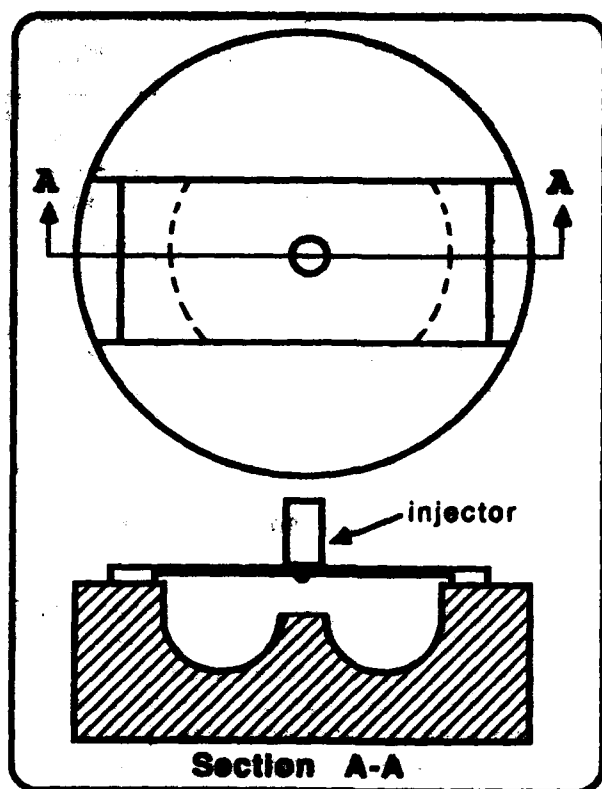


Fig. 4a. Top and section views of truncated piston used in photographic study.

as the numerical predictions. In this figure and the following figures, the radial outline of the piston bowl is shown as the narrow outline from the model results, while the thick line indicates the truncated bowl outline as seen by the camera (see Fig. 4a). The spray outline is shown for the frame obtained 0.8 ms after the start of injection for the fuel rail pressure of 6.1 MPa. As is evident from the figure, this "standard" model does not accurately predict the general spray shape. The predicted spray shows little dispersion of the drops relative to the photographic results, and considerably over predicts the penetration of the spray cloud. There are several possible explanations for this disagreement. Most arise from the fact that in previous work, near field drop behavior was not a major interest, and therefore was not considered in evaluating the accuracy of the results. For this application, near field effects will clearly have a major impact.

In order to improve the results of the standard model, three modifications were proposed. These modifications were not intended to be conclusive, but were intended to indicate the parametric variation and sensitivity of the current model to small modifications in order to improve near field predictions. Conclusive development of these submodel improvements will require more detailed experimental data than is currently available.

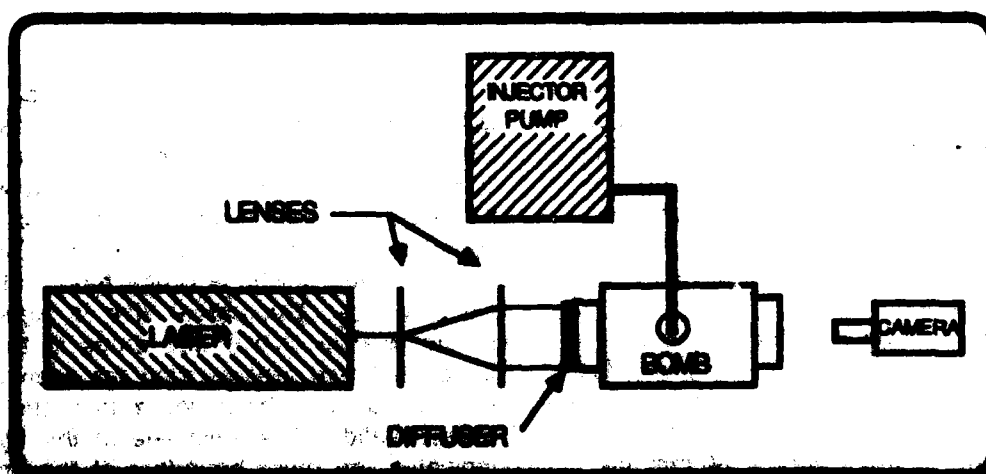


Fig. 4b. Equipment layout used in photographic study.

The first of the proposed modifications was to alter the size of the drops as they emerge from the orifice at the exit of the fuel injector. As had been noted [2] for far field comparisons, choosing a single initial drop size as the orifice diameter gave reasonably good agreement for downstream drop size and velocity for dense, solid cone sprays. Since near field conditions do not provide the length required for the combination of drop breakup and coalescence to obliterate the initial spray conditions, initial conditions are likely to be much more important. For this numerical experiment, an initial drop diameter an arbitrary 1/5 the diameter of the exit orifice (80 μm) was chosen. The results for this calculation are shown in Fig. 5b. The model predictions are compared with the experimental spray outline for a fuel rail pressure of 6.1 MPa at 0.8 ms after the start of injection. This figure of the drop parcel locations still does not agree well with the spray shape from the photograph, however some effects not seen in the standard case become evident. These include a number of drops which are entrained in the induced gas flow. Because of their small size and low momentum, these drops do not hit the spray impingement surface. The overall spray pattern still considerably under predicts the lateral spread of the spray cloud, but does come much closer to predicting the spray penetration accurately.

A second numerical experiment to vary the initial drop size description was tested using an initial drop size distribution as proposed in the original KIVA model (Eqn. 1) with an average Sauter mean diameter (SMD) of 50 μm . The results for this calculation are shown in Fig. 5c. As with the previous numerical experiment, all other conditions were held constant in order to determine the effect of the initial drop size description on the overall spray profile. The model results are compared with the experimental results at a fuel rail pressure of 6.1 MPa, 0.8 ms after the start of injection. This modification produces results which are very similar to the results for the case of drops which had an initial diameter of 1/5 the orifice diameter. The spread of the drops is less than experimentally observed, but the penetration depth of the spray is reasonably good.

While it is quite likely that a more detailed description of the injection drop size is required, it is equally clear that modest modifications of this parameter alone will not produce good agreement with the photographic record.

A second set of modifications to the standard model was a set of modifications describing the change in the spray characteristics due to the near field impact of the spray on the solid surface. These modifications included changing the drop size due to the collision with the solid wall, and modification of the velocity vector of the drop parcels after collision with the wall. The first of these numerical experiments was based on the proposal that in the near field with high velocity liquid, impact with a solid wall is likely to have a major effect on the drop size distribution. Previous work for far field wall interactions described the resulting drop trajectory, but assumed the drop size remained unchanged in the collision [5]. For the conditions considered in that problem, the assumption seemed justified by reasonably good agreement with some quantitative and some qualitative data. For the high velocity near field liquid, it seems probable that the drop size distribution is significantly altered by the impact, generating many more small drops than would exist without the impact. This effect was qualitatively indicated by the results of Wachters and Westerling [11] who showed large water drops at approach Weber numbers of 184 break up into many smaller drops at a surface. In an attempt to simulate the effect of change in drop size distribution due to wall impact, a numerical experiment was run using the standard model description for the initial drop sizes, and allowing all drops which hit the surface to immediately break into drops 1/5th the size of the drops before impingement, with mass and kinetic energy conserved. As with the previous models described, the trajectories of these drops were determined by the jet analogy model of Reitz and Naber. As seen in Fig. 5d, this modification does have a significant impact on the drop parcel distribution, but when compared with the photographic results, it under predicts the rate of lateral spread, while predicting the penetration depth reasonably well.

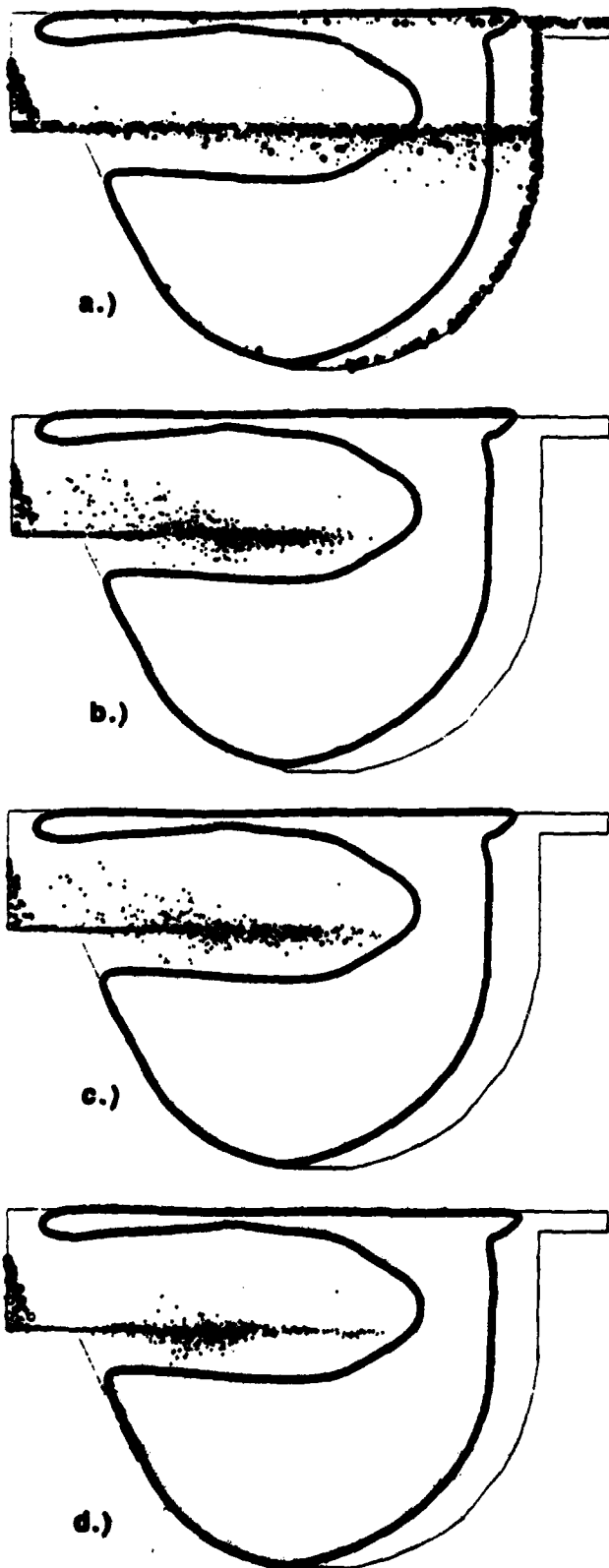


Fig. 5. Comparison of the experimental spray outline (bold line) for the medium rail pressure case (6.2 MPa) at 0.8 ms after the start of injection vs. the predictions of

- a.) the "standard" model
- b.) an injected drop dia. 1/5th orifice dia.
- c.) an injected drop dia. distribution ($r_{32}=25\mu\text{m}$)
- d.) an impinged drop dia. reduced by 1/5th.

The final modification applied to the standard model was to incorporate a component of velocity normal to the surface in the drop trajectory for each drop that hits the surface. The drop impingement model of Reitz and Naber allows drops which hit the surface to leave tangent to the surface in a direction relative to the plane of incidence calculated using Eqns. (5) and (6). For near field high velocity sprays, it is likely that some component of velocity normal to the surface is generated by the impingement. Detailed information on the effects of drop impingement at high Weber number ($We = \rho v^2 d / \sigma$) conditions is scarce. Wachters and Westerling [11] provided some data and high speed photographs for single water drops impinging on a heated surface for incoming Weber numbers up to 184. The Weber number in the current set of experiments is much higher, greater than 1000. Although the data presented in Wachters and Westerling is primarily for heated surfaces, at the high Weber numbers cited, the heated surface should have little impact for drops which wet the surface. The data of Wachters and Westerling indicated that for high incoming Weber number drops, a single large drop immediately shatters into many smaller drops. Their photographs (Fig. 11 of [11]) indicated that many of these smaller drops rebound from the surface with a small velocity normal to the surface. A summary plot from Wachters and Westerling (Fig. 7 of [11]) suggests that for high incoming drop Weber numbers, relatively low rebound Weber numbers are produced, however, this plot represents single drop impingement and rebound, without subsequent

breakup. Although the data of Wachters and Westerling is for incoming Weber numbers much lower than those of the current work, the qualitative description of the drop breakup and rebound is accepted. It is not clear exactly what form the normal reflected velocity should have. For this exploratory study, the normal component of drop velocity after impingement was randomly chosen to be between 0 to 34% of the incoming velocity. The tangential velocity orientation was determined as before from Eqns. (5) and (6). The drop size was reduced to 1/5th of the impinging drop size. The number of drops in the parcel was chosen to conserve mass and the tangential velocity magnitude was chosen to conserve kinetic energy. The results of these modifications are shown in Figs. 6, 7, 8, and 9. These results represent the best agreement of the model modifications with the photographic data for the limited range of model modifications used.

Figure 6 shows the set of five spray contours taken from the photographs for the fuel rail pressure of 4.7 MPa and peak injection pressure of 83 MPa. The figures represent times from the start of injection of 0.2, 0.4, 0.6, 0.8, and 1.0 ms. The model predictions for the same injector conditions and time intervals are superimposed on the spray outlines. The agreement between the two is reasonably good, although at early times after the start of injection the model appears to over predict the spray penetration. Figure 7 shows the five spray contours for a fuel rail pressure of 6.1 MPa, a peak injection pressure of 91 MPa, for the same time intervals as in the previous test. Again, the data are compared with the numerical model using the modifications for surface drop breakup and normal velocity. The comparisons again show relatively good agreement, with somewhat better agreement for the spray penetration at early times in the injection. Figure 8 shows the five spray contours for the fuel rail pressure of 7.8 MPa and peak injection pressure of 116 MPa. Using the same time intervals as in the previous figures, the data are compared with the numerical model for these input conditions. The comparison of the experimental spray outline and the predicted parcel locations shows reasonably good agreement between the model and the experiment for this set of operating conditions

in the current geometry. As for the low fuel injection pressure case, the spray penetration is somewhat over predicted at early times after the start of injection. Figure 9 summarizes the results from the photographs and model predictions by comparing the calculated radial penetration of the spray verses time (indicated by the lines) for the three rail pressures studied (4.7, 6.1, and 7.75 MPa) with the results from the photographs (indicated by the symbols).

It should be noted that there remains some ambiguity in the results, due to characteristics of the experimental results and the numerical results. The experimental results consist of the high speed movies of the back-lit spray pattern. The start of injection could not be determined exactly because of the limited frame rate of the camera. For comparison with the models predictions it was assumed injection started one frame (0.2 ms) before the first appearance of the spray. Since the pattern is so dense, spray density variations are not clearly seen. The photographic results show a generally very dense cloud of spray which spreads across the piston bore with time. Since the photographs represent a line-of-sight average attenuation of the incident light, the visualized "cloud" may be a uniform cloud with the outline indicated, or more likely, a cloud with a thinner center section as indicated by the model, and a thick outer edge where the slow drop velocities allow for increased lateral spread of the spray pattern. For sufficiently dense spray clouds, these two situations are not distinguishable with the experimental technique currently employed.

It should also be emphasized, that in applying each of the suggested modifications to the standard model, some arbitrary choices were made as to relative initial drop size, or drop size after surface impact, or normal drop velocity after surface impact. There exists very little data under the conditions of interest for detailed analysis of these aspects of the problem. One objective here was to evaluate which mechanisms appear to be most likely to play a major role in the problem using some reasonable but arbitrary assumptions. Subsequent detailed experiments will hopefully allow detailed modeling of those mechanisms which appear to be most significant.

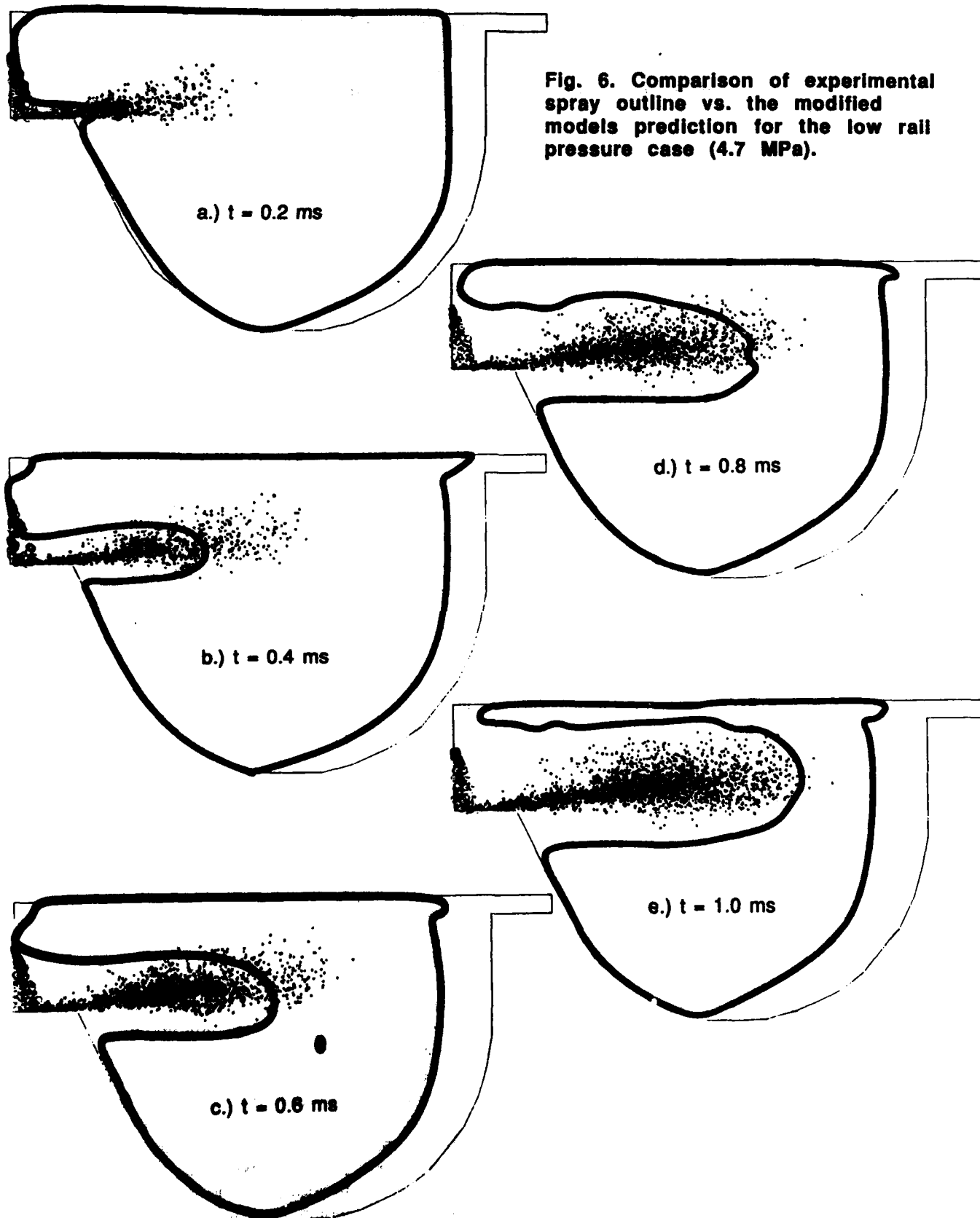


Fig. 6. Comparison of experimental spray outline vs. the modified models prediction for the low rail pressure case (4.7 MPa).

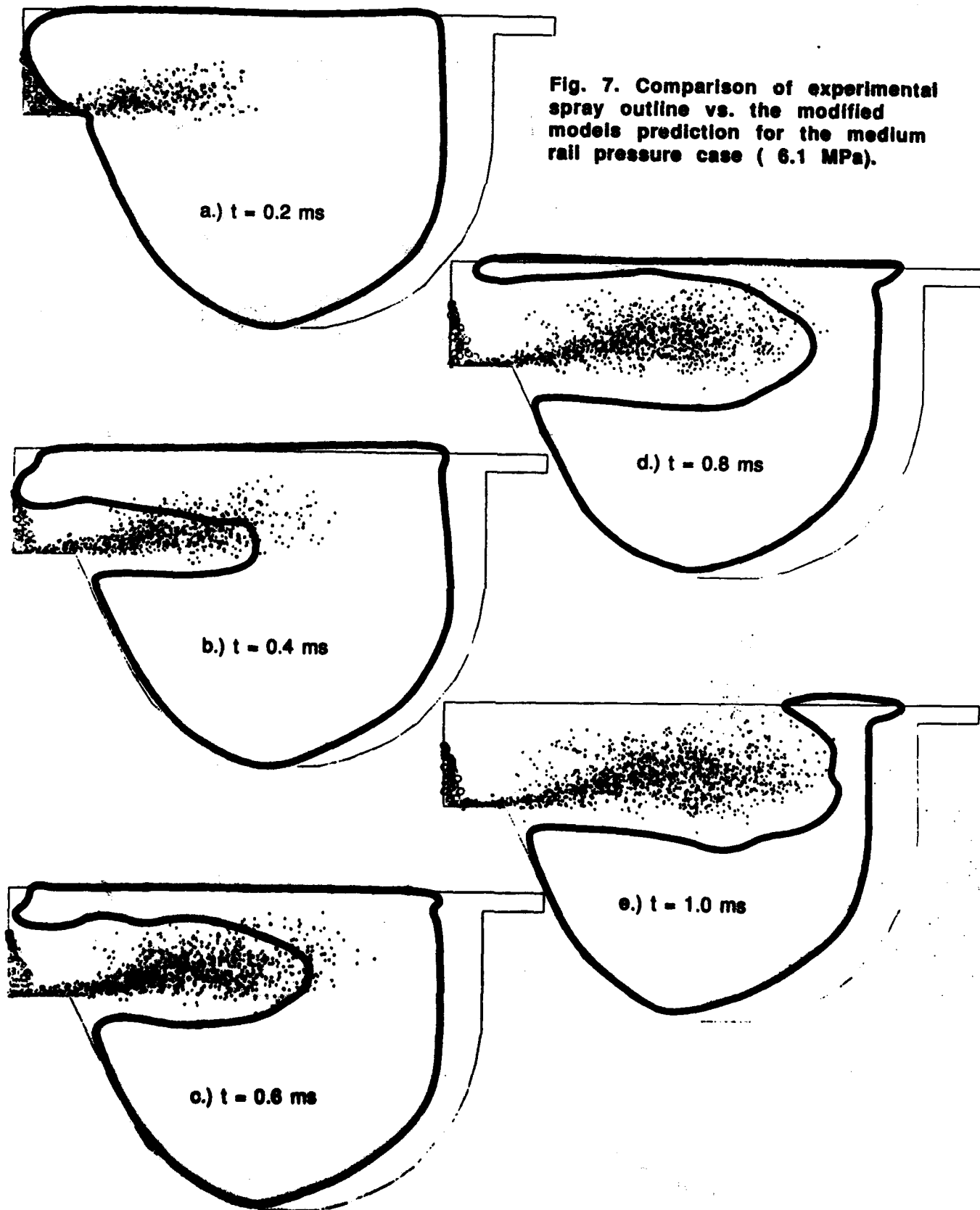


Fig. 7. Comparison of experimental spray outline vs. the modified models prediction for the medium rail pressure case (6.1 MPa).

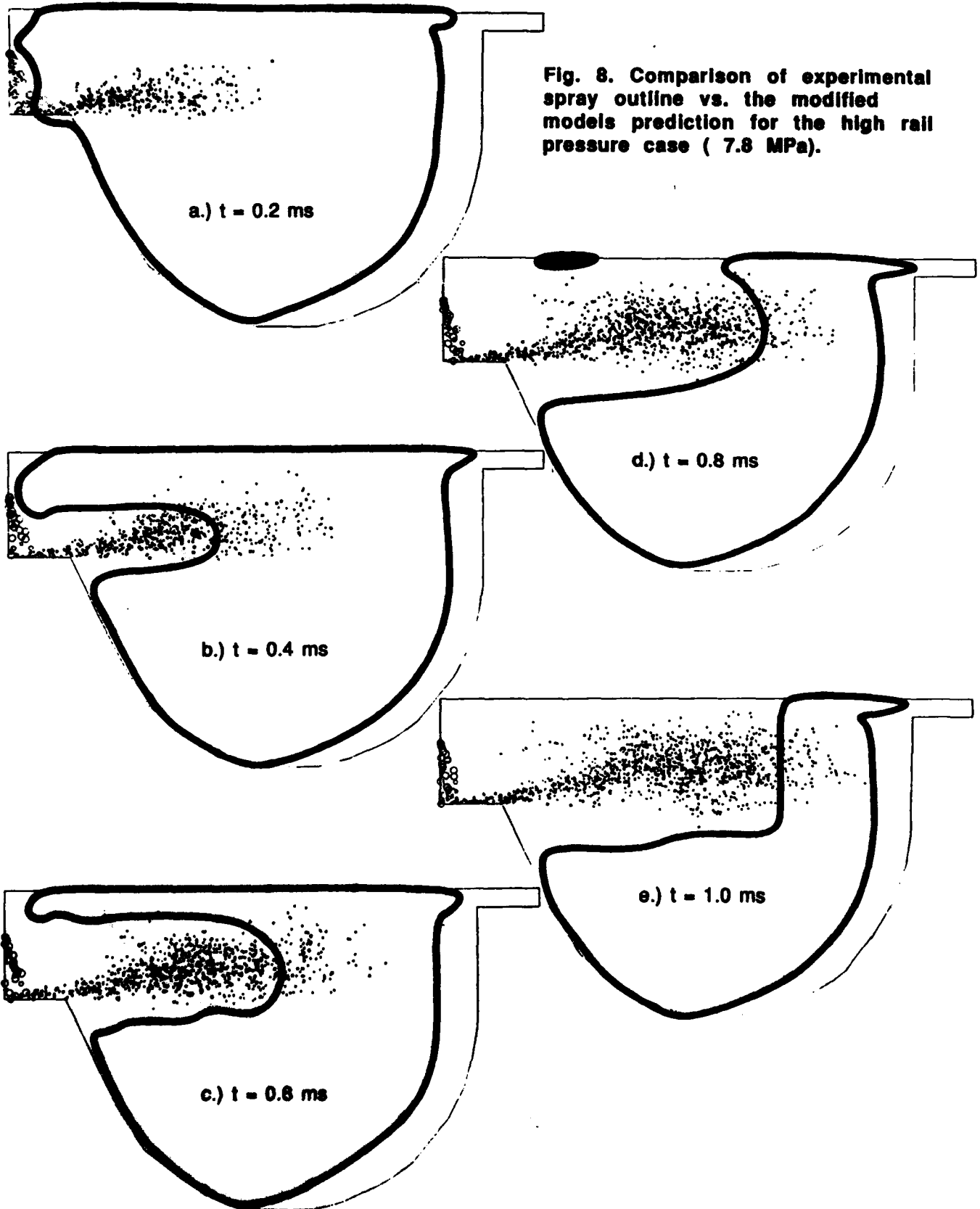


Fig. 8. Comparison of experimental spray outline vs. the modified models prediction for the high rail pressure case (7.8 MPa).

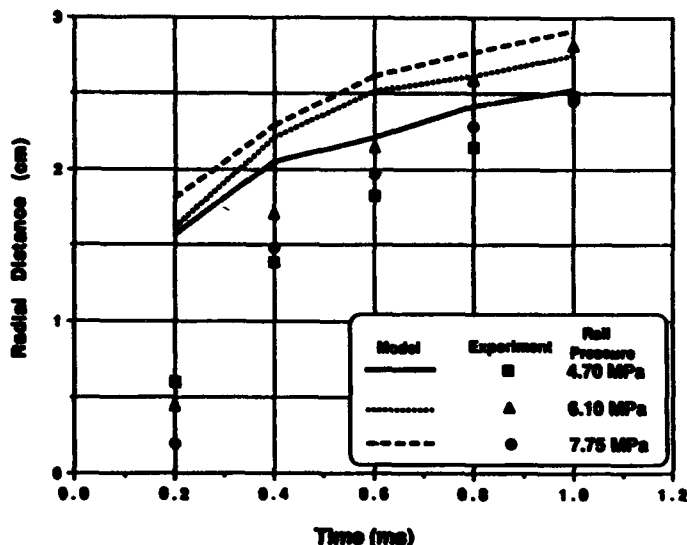


Fig. 9. Comparisons of the experimental impinged spray penetration vs. the modified models predictions at the three rail pressures as a function of time.

SUMMARY

A series of experiments were performed in a cold high pressure constant volume bomb using a single hole fuel injector spray impinging onto a land in the middle of a piston bowl. The overall spray pattern was recorded as a function of time, and compared with the results of a numerical spray model. After the model was modified by including estimates of the surface interaction effects on drop size and normal velocity, agreement between the experiment and model was reasonably good. The indication from this result is that the current "standard" model does not do a good job of predicting spray impingement on a solid surface near the fuel injector. Minor modification of the current model improves this agreement. Detailed modeling to account for this improvement awaits more detailed data on drop sizes and velocities near solid surfaces in the near field of the injected spray.

ACKNOWLEDGEMENTS

The authors wish to acknowledge the support of the Army Research Office through the designation of the University of Wisconsin-Madison as the Center of Excellence for Advanced Propulsion Systems. Computer support for this project was provided by the San Diego Supercomputer Center, San Diego, Ca.

NOMENCLATURE

d	orifice diameter
$g(r)$	drop probability distribution
l	distance from nozzle tip
P	pressure
r	drop radius
r_{32}	Sauter mean drop radius
V	velocity
α	impingement angle relative to surface normal
β	probability parameter
ρ	density
σ	surface tension
ν	kinematic viscosity
ψ	azimuthal surface angle

subscripts

g	gas
rel	relative gas - drop

REFERENCES

1. Amsden, A.A. Ramshaw, J.D., O'Rourke, P.J. and Dukowicz, J.K., "KIVA: A Computer Program for Two- and Three-Dimensional Fluid Flows with Chemical Reactions and Fuel Sprays," Los Alamos Report No. LA-10245-ms, February 1985.
2. Reitz, R.D. and Diwakar, R., "Effect of Drop Breakup on Fuel Sprays," SAE Paper 880489.
3. O'Rourke, P. J. and Amsden, A. "The TAB Method for Numerical Calculation of Spray Droplet Breakup," SAE Paper 872089.
4. O'Rourke, P. J., and Bracco, F. V., "Modeling of Drop Interactions in Thick Sprays and Comparison with Experiments," Institution of Mechanical Engineers(1980).
5. Naber, J.D. and Reitz, R.D., "Modeling Engine Spray/Wall Impingement," SAE Paper 880107.
6. Kroeger, C. A., "A Neat Methanol Direct Injection Combustion System for Heavy Duty Applications," SAE Paper 881189.

7. Kato, S. and Onishi, S., "New Mixture Formation Technology of Direct Injection Stratified Combustion SI Engine (OSKA)," SAE Paper 871689.

8. Reitz, R.D. and Dwekar, R., "Structure of High-Pressure Sprays," SAE Paper 870598.

9. Johnson, W. "Calibration Test Report, Servojet Injector for University of Wisconsin, Single-Shot Combustion Bomb Testing," MR-349, BKM, January 1988.

10. Wahl, F. M., Digital Image Signal Processing, (Artech House, Boston) 1987.

11. Wachtors, L. H. J. and Westerling, N. A. J., "The Heat Transfer from a Hot Wall to Impinging Water Drops in the Spheroidal State," Chem. Eng. Sci. 21, 1047-1056(1966).